Communications

Time–Frequency Distribution Analysis of Scattering from Waveguide Cavities

Ali Moghaddar and Eric K. Walton

Abstract— **Time–frequency distributions (TFD) describe a signal in terms of its joint time and frequency content. In this paper, the TFD analysis of the electromagnetic scattering from a circular waveguide cavity is investigated. Two time–frequency representations, the Wigner distribution and the running-window Fourier transform, are applied to the frequency-domain scattering data and the results are compared. For the cavity, propagating modes and cutoff frequencies can be determined from the TFD, whereas neither time nor frequency representations will directly provide such information.**

I. Introduction

In the analysis of wideband electromagnetic scattering, it is common to obtain time-domain profiles by an inverse Fourier transform (IFT) of the frequency response. This gives an approximation of the impulse response of the scatterer. In some applications, it is natural to discuss different scattering features in the frequency-domain, whereas in other applications, the time-domain response is more appropriate. Sometimes, however, it may be desirable to examine the mathematical and physical properties of the scattering as a function of time and frequency simultaneously. This is especially important for frequency dispersive scattering such as some radar absorbing materials (RAM's) or frequency dispersive structures such as ducts or inlets.

For nondispersive scattering, the local maxima of the time-domain response correspond to local scattering features, such as corners, edges, or specular reflections [1]. For frequency dispersive features, the corresponding impulse response will be spread in the time domain. Because of this time spread, it may not be possible to associate such a response to a spatially local feature of the scatterer. In such cases, the impulse response alone cannot directly provide information about the dispersive characteristics of the individual scattering mechanisms.

In this paper, the electromagnetic (EM) scattering from waveguide cavities is examined as an example of frequency dispersive scattering. It will be shown that time–frequency distributions (TFD's) provide a meaningful representation of the dispersive mechanism. Two time–frequency representations, the running window Fourier transform and the Wigner distribution, are applied to the scattering from waveguide cavities. For the waveguide cavity, propagating modes and cutoff frequencies can be readily determined from the TFD, whereas neither time nor frequency representations will directly provide such information.

II. TFD of a Circular Waveguide Cavity

As an example of frequency dispersive scattering, let us consider the EM scattering from a waveguide cavity. Referring to Fig. 1, one can write the total scattered field as

$$\vec{E}^s = \vec{E}^s_{\text{rim}} + \vec{E}^s_{\text{cav}} + \vec{E}^s_{\text{ext}}, \tag{1}$$

Manuscript received December 23, 1991; revised February 1, 1993. This work was supported by the Ohio State University ElectroScience Laboratory Compact Range Consortium.

The authors are with the ElectroScience Laboratory, Ohio State University, Columbus, OH 43212.

IEEE Log Number 9209215.

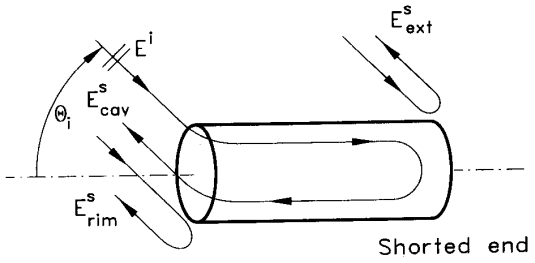

Fig. 1. Geometry of the open-ended circular cavity and major scattering mechanisms.

where $\vec{E}_{\text{rim}}$ is the field scattered by the edge of the aperture at the open end of the cavity, and $\vec{E}^s_{\text{ext}}$ is the scattering from the exterior of the cavity. The scattering from the interior of the cavity, $\vec{E}^s_{\text{cav}}$, is the dominant frequency dispersive part of the total scattered signal. For frequencies below the cutoff frequency of the cavity, $\vec{E}^s_{\text{cav}}$ does not contribute to the total scattering. As the operating frequency increases, the number of propagating modes and the propagation constant for each propagating mode increase. As a result, the total scattering from the cavity is frequency dispersive. In the following subsections, the scattering from a circular cavity is considered for normal incidence and for 45° incidence cases.

A. Normal Incidence Case

A 2-ft (61 cm) long, 1.75-in. (4.44 cm) diameter circular cavity with an open end (see Fig. 1) is considered. The scattered signal is measured (in units of radar cross section converted to normalized voltage with relative phase) from 2 to 18 GHz at normal incidence ($\theta = 0$). The band-limited impulse response is computed using an IFT of the windowed 2–18 GHz data [1]. The magnitude of the measured frequency data and the band-limited impulse response are shown in Fig. 2. From this figure, the scattering from the leading and trailing ends of the cavity can be seen at −2.0 and 2.0 ns, respectively. From the impulse response, one can also see a response spread in time feature after 2.0 ns. This can be an indication that resonant scattering from the cavity is present. However, neither the frequency nor the time-domain data of Fig. 2 provide specific information about the frequency dispersive features of the cavity.

For comparison, theoretical scattering data were also computed using a high-frequency modal approach [2]. In computing the theoretical data, only the scattering from the rim, $\vec{E}^s_{\text{rim}}$, and scattering from the interior of the cavity, $\vec{E}^s_{\text{cav}}$, are included. The band-limited impulse response for the theoretical data is included in Fig. 2.

To show the frequency-dispersive behavior of the cavity, the running window Fourier transform [3] (RWFT) is computed from the complex scattering data $S(\omega)$ such that

$$\text{RWFT}_s(t, \omega) = \int_{-\infty}^{\infty} S(\Omega) W(\omega - \Omega) e^{j\Omega t}\, d\Omega, \tag{2}$$

where a 2-GHz-wide Kaiser–Bessel window has been used for the $W(\omega)$. The magnitude of the distribution, $|\text{RWFT}_s(t, \omega)|$, is shown in gray-scale levels in Fig. 3. In the same figure, along the time and frequency axes, the impulse response, and the magnitude of

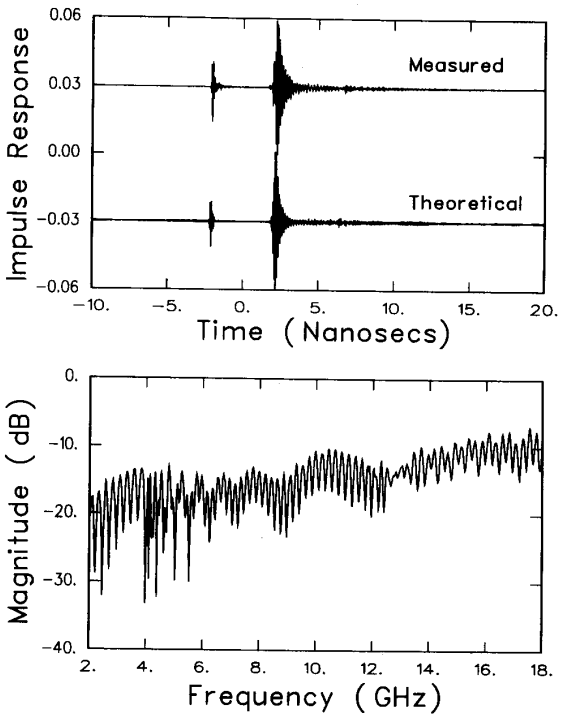

Fig. 2. Magnitude of the measured frequency scan data, and the band-limited impulse response for measured and theoretical data (0° incidence, horizontal polarization).

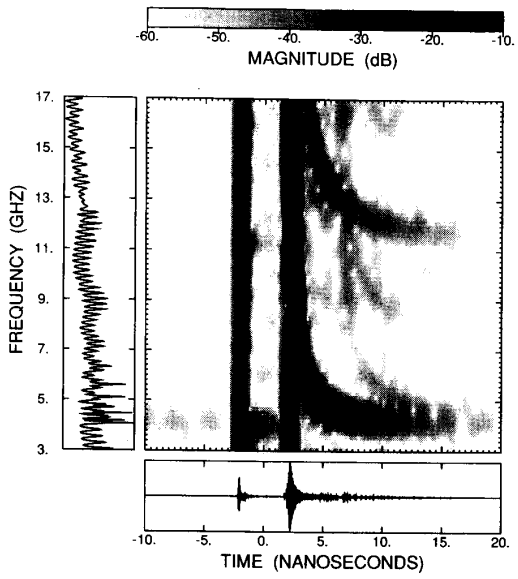

Fig. 3. Running-window Fourier transform time–frequency distribution using a 2-GHz-wide Kaiser–Bessel window. Measured data for the 1.75-in-diameter circular cavity, horizontal polarization, 0° incidence.

the frequency response are also included. From the TFD, one can identify the leading and trailing ends of the cavity, and the two cutoff frequencies at 3.9 GHz and 11.3 GHz. These values correspond to

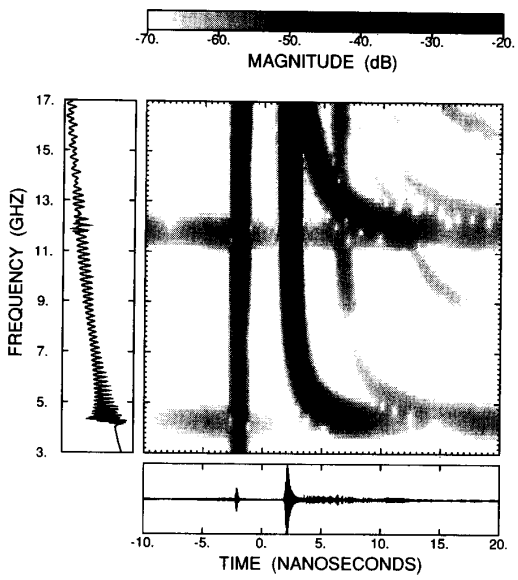

Fig. 4. Running-window Fourier transform time–frequency distribution using a 2-GHz-wide Kaiser–Bessel window. Theoretical data for the 1.75-in.-diameter circular cavity, horizontal polarization, 0° incidence.

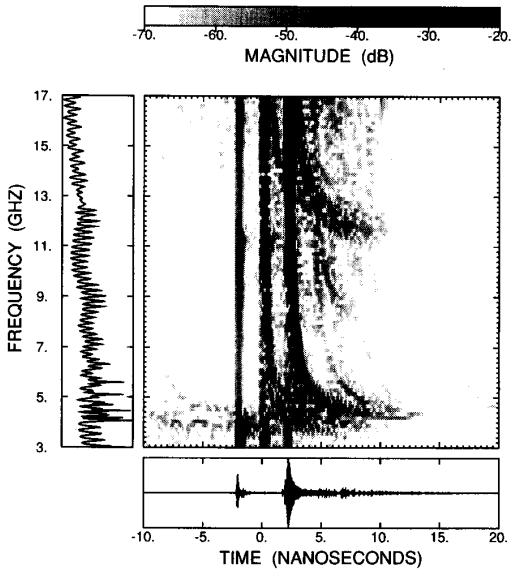

Fig. 5. Wigner time–frequency distribution for the measured data.

the cutoff frequencies for the TE_{11} and TE_{12} modes of the 1.75-in.-diameter circular cavity.

The shape of the response caused by each mode in the time–frequency plane also indicates the variation of the propagation constant with frequency. As the operating frequency is increased, the propagation constant of individual modes approaches the free-space propagation constant. Thus, for each mode, the time delay corresponding to the reflection from the closed end approaches the time delay corresponding to the exterior trailing end scattering. The

TABLE I
CUTOFF FREQUENCIES FOR A 1.75-IN.-DIAMETER OPEN-ENDED CIRCULAR CAVITY

Mode	TE_{11}	TM_{01}	TE_{21}	TM_{11} TE_{01}	TE_{31}	TM_{21}	TE_{41}
f_c (GHz)	3.95	5.17	6.56	8.23	9.02	11.03	11.42
Mode	TE_{12}	TM_{20}	TM_{13}	TE_{51}	TE_{22}	TE_{20} TM_{12}	
f_c (GHz)	11.45	11.86	13.70	13.78	14.41	15.07	

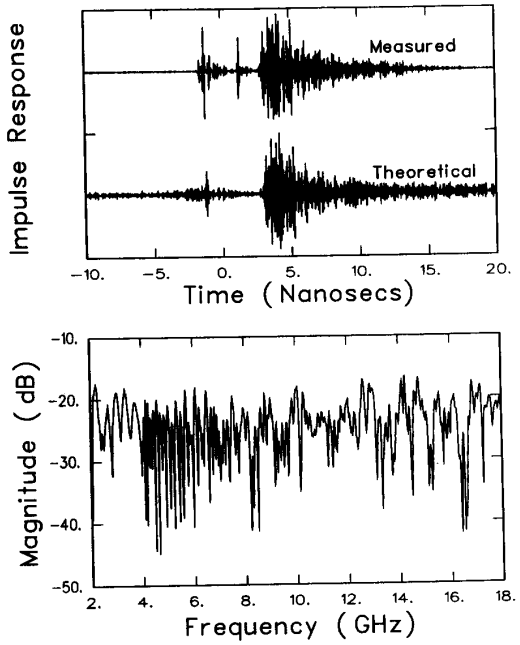

Fig. 6. Magnitude of the measured frequency scan data, and the band-limited impulse response for measured and theoretical data (45° incidence, horizontal polarization).

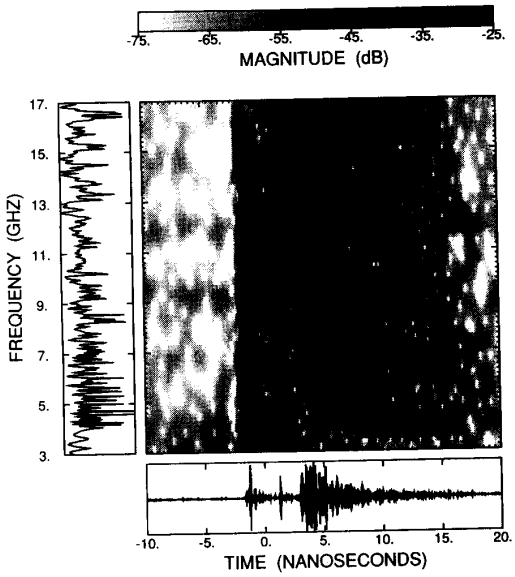

Fig. 7. Running window Fourier transform time–frequency distribution for the measured data (1.75-in.-diameter circular cavity, horizontal polarization, 45° incidence).

hook-shaped curves in the T–F plane are a result of this variation in the propagation time.

The TFD for the theoretical data using the RWFT is shown in Fig. 4. By comparing Figs. 3 and 4, one can see that the cutoff frequencies and the general shape of the distribution for the measured and theoretical data are very similar. From the TFD of the measured data, one can see the external scattering from the trailing end of the cavity at a constant time (2 ns) for all frequencies. However, for the theoretical data, since the scattering from the exterior is not included, the cutoff for the TE_{11} mode (3.9 GHz) is the starting frequency where the effect of the closed end can be observed. It is worth emphasizing that this information cannot be obtained by comparing the impulse responses in Fig. 2.

Another difference between the TFD of the theoretical data and the TFD of the measured data is the resonance behavior at the cutoff frequencies for the theoretical data. At the two cutoff frequencies, an apparent noncausal response can be observed for the theoretical case only. This is actually due to the aliasing of a very late time response which is folded into the early time region. This implies that the theoretical model should have included some attenuation for the internal propagating modes.

The second TFD technique applied to the cavity data is the Wigner distribution. The Wigner distribution (WD) of the scattering data, $S(\omega)$, can be computed by [4]

$$\mathrm{WD}_s(t, \omega) = \int_{-\infty}^{\infty} S\left(\omega + \frac{\Omega}{2}\right) S^*\left(\omega - \frac{\Omega}{2}\right) e^{j\Omega t}\, d\Omega. \quad (3)$$

It has been shown [5] that the Wigner distribution has the highest signal concentration in the time–frequency plane. The Wigner distribution for the measured data is shown in Fig. 5. As expected, the Wigner distribution provides a higher resolution for the leading and trailing ends of the cavity as well as the propagating modes. The major disadvantage of the Wigner distribution is the presence of nonphysical cross terms [3]. These nonphysical cross terms can be ignored during the interpretation of the TFD if they can clearly be identified. For some sections of the distribution, however, the cross terms obscure the distribution to the point where it is difficult to distinguish between the co- and cross components.

B. 45° Incidence Case

In the second experiment, the backscattering from the cavity was measured at a 45° azimuth angle. The magnitude of the measured signal and the band-limited impulse response for horizontal polarization are shown in Fig. 6. From the impulse response in this figure, one can identify the leading and trailing ends of the cavity. However, no specific information about the propagating modes or cutoff frequencies is available directly from the impulse response. The theoretical frequency data were also computed for 45° incidence.

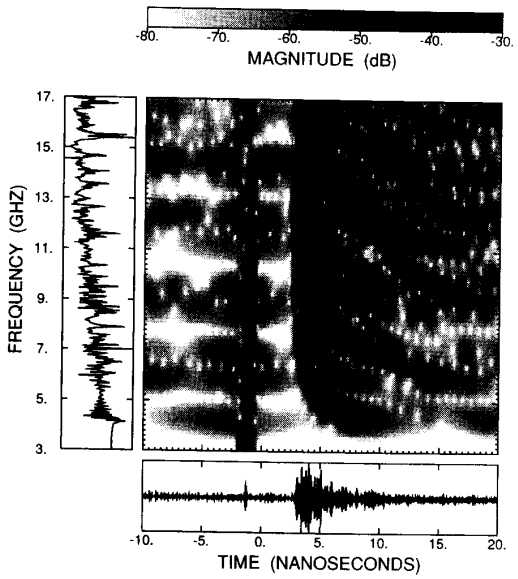

Fig. 8. Running window Fourier transform time–frequency distribution for the theoretical data (1.75-in.-diameter circular cavity, horizontal polarization, 45° incidence).

Since scattering from the exterior is not included in the theoretical data, scattering from the trailing end of the cavity will be absent (compare the impulse response at +1 ns for theoretical and measured data in Fig. 6).

The TFD's obtained by applying the running-window Fourier transform to the measured and theoretical data are shown in Figs. 7 and 8, respectively. From these figures, a number of propagating modes can be seen. The cutoff frequencies for the propagating modes of the cavity are also computed and the results are summarized in Table I. By comparing the TFD in Fig. 7 with Table I, one can identify the particular modes which contribute to the total scattering.

III. Conclusions

In this paper, time–frequency distributions (TFD) have been used to evaluate the EM scattering from waveguide cavities. As an example, the TFD of measured and theoretical backscattering from a 1.75-in.-diameter circular cavity were examined. Two time–frequency representations, the running window Fourier transform (RWFT) and the Wigner distribution (WD), were compared. It was shown that for the cavity, the dominant propagating modes can be determined from the TFD, whereas neither time nor frequency representations will directly provide such information.

References

[1] E. K. Walton and J. D. Young, "The Ohio State University compact radar-cross section measurement range," *IEEE Trans. Antennas Propagat.*, vol. 32, pp. 1218–1223, Nov. 1984.

[2] C. W. Chuang and P. H. Pathak, "Ray analysis of modal reflection for three-dimensional open-ended waveguides," *IEEE Trans. Antennas Propagat.*, vol. 37, pp. 339–346, Mar. 1989.

[3] L. Cohen, "Time–frequency distributions—A review," *Proc. IEEE*, vol. 77, no. 7, pp. 941–981, 1989.

[4] T. A. C. M. Claasen and W. F. G. Mecklenbrauker, "The Wigner distribution—A tool for time–frequency signal analysis; Part I: Continuous-time signals," *Philips J. Res.*, vol. 35, no. 3, pp. 217–250, 1980.

[5] D. Gabor, "Theory of communication," *J. Inst. Elec. Eng.*, vol. 93, pp. 429–441, 1946.

Impedance Matching of a Dual-Frequency Microstrip Antenna with an Air Gap

Choon Sae Lee and Vahakn Nalbandian

Abstract—**A novel microstrip antenna has been proposed to operate at dual frequencies. The microstrip is a single layer patch with nonradiating edges closed with a conducting foil. Resonant frequencies are altered by varying the air gap under the patch. The separation of the resonant frequencies can be nearly zero and has no upper limit in principle. The input impedance is easily matched by shifting the air gap. The radiation patterns are not affected by modification for dual-frequency operation.**

I. Introduction

Microstrip antennas have many advantages over the conventional antennas, for example, in weight, cost, and profile. The most detrimental aspects of the microstrip antennas, which limit more widespread usage, are in their inherent narrow bandwidth. The most popular technique to obtain a larger bandwidth is either to place parasitic elements next to the radiating element or to stack them vertically [1]–[3]. When the operating frequencies are widely separated, such techniques may not provide sufficient bandwidth. In some applications, such as in the global positioning system (GPS), only a few distinct frequency bands are needed as opposed to a continuous operating frequency range. The purpose of this paper is to introduce a novel dual-band microstrip antenna. This device relies upon a single dielectric layer instead of the widely used two-layer structure [4], [5]. The radiation pattern of the new device is nearly identical to that of the single-band microstrip antenna and the design procedure is relatively simple.

Section II presents the design scheme for desired resonant frequencies. The input impedance is matched at both resonant frequencies by varying the feed location and the air gap size and location. Experimental results are given in Section III.

II. Design Scheme

The proposed microstrip antenna is shown in Fig. 1. The layer thickness is assumed to be small compared with the wavelength, and the cavity model [6], [7] is used for the design scheme. The microstrip antenna is considered to be a lossy resonating cavity enclosed by a perfect electric conductor for the metallic surfaces and a perfect magnetic conductor for the radiating edge. A characteristic equation for the resonant frequencies is obtained by imposing the boundary conditions and the continuity conditions of the fields at the

Manuscript received April 23, 1992; revised October 30, 1992.

C. S. Lee is with the Electrical Engineering Department, Southern Methodist University, Dallas, TX 75275.

V. Nalbandian is with the U.S. Army CECOM, Intelligence and Electronic Warfare Directorate, Fort Monmouth, NJ 07703.

IEEE Log Number 9209216.